Filter Bank-based Multicarrier Modulation for Multiple Access in Next Generation Satellite Uplinks: A DVB-RCS2-based Experimental Study

Vassilis Dalakas, Eleftherios Kofidis

Filter Bank-based Multicarrier Modulation for Multiple Access in Next Generation Satellite Uplinks: A DVB-RCS2-based Experimental Study

Vassilis Dalakas and Eleftherios Kofidis

Abstract—**In the context of the on-going evolution of satellite communication systems to their next generation, involving higher data rates and increased flexibility, it is of interest to study in depth the applicability of multiple access (MA) multicarrier modulation (MCM) schemes that have shown promise to meet the requirements of the future terrestrial networks. A comparative study of MA schemes employing offset quadrature amplitude modulation (OQAM)-based filter bank multicarrier (FBMC/OQAM) and classical orthogonal frequency division multiplexing (OFDM) is presented in this paper. The considered air-interface follows the latest Digital Video Broadcasting (DVB) family of standards for the satellite return link. Considering a high-power amplifier (HPA) of a very small aperture terminal (VSAT), the performance of the two MA schemes is evaluated in an asynchronous multi-user satellite environment involving time and frequency synchronization errors. Our results indicate that while FBMC-based MA (FBMA) is more sensitive near saturation and in the presence of timing errors, it is more robust to frequency offset errors not only in terms of the Total Degradation (TD) but also in terms of the Spectral Efficiency (SE), since it only needs minimal guard bands among the different users. This is a preliminary study of the potential gains from the integration of the FBMA technology in the satellite infrastructures and standards. Future work will include results on single-carrier modulation (SCM) FBMA as well.**

Index Terms—**Digital Video Broadcasting via Satellite, Filter Bank Multicarrier Multiple Access, Inter-Block Interference, Orthogonal Frequency Division Multiple Access, Satellite Uplink, Total Degradation.**

I. Introduction

The ever increasing commercial demand for higher user data rates via satellites has led to the adoption of the 2nd Generation Digital Video Broadcast Return Channel via Satellite (DVB-RCS2) [1] system. This standard, designed by the Digital Video Broadcasting (DVB) project, defines the complete air interface specification for two-way satellite broadband very small aperture terminals (VSATs). Low cost VSAT equipment can provide highly dynamic, demand-assigned transmission capacity to a broad range of users, while DVB-RCS2 provides users with broadband internet connection, without requiring any local terrestrial infrastructure [2].

Nevertheless, the potential integration with the terrestrial infrastructure, allowing vertical handover to terrestrial radio interfaces and ground-controlled software defined radio [3], has been recently receiving increasing attention in view of the trend towards the future '2020 and beyond' internet supporting Tbit/s traffic [4]. The European Satellite Agency (ESA), through its Advanced Research in Telecommunications Systems (ARTES)–1 program, has identified several key issues concerning the progress to the High Throughput Satellites (HTS) [3] of Tbit/s capabilities [5]. In this context, developments that parallel the evolution to 5th generation (5G) terrestrial systems have also been under study in satellite communications [3], [6].

The selection of an appropriate multi-carrier modulation (MCM) and multiple access (MA) scheme plays a key role in this direction [7][1]. Orthogonal frequency division multiplexing (OFDM) is used in several well known standards, including the 2nd Generation of Terrestrial DVB (DVB-T2), the DVB by Satellite Handheld (DVB-SH) [9] and the 3rd Generation Partnership Project (3GPP) Long Term Evolution (LTE) standard [10]. Among the reasons for its wide adoption are its robustness to channel multipath (though at the cost of the cyclic prefix (CP) redundancy) and its conceptual and implementation simplicity. Orthogonal Frequency Division Multiple Access (OFDMA) is the MA scheme that naturally extends OFDM to simultaneously serve multiple users [11]. Despite its many advantages, however, OFDM(A) has been seriously questioned as to its suitability to meet the increased requirements of future communication systems for flexibility, spectral and power efficiency, and high robustness to synchronization errors, among others [7]. Alternative MCM schemes, which show a potential to meet these requirements, have thus been studied and are based on the use of filter banks for modulation and demodulation [7]. Filter bank-based multicarrier (FBMC) systems using offset quadrature amplitude modulation (OQAM) (also known as FBMC/OQAM or OFDM/OQAM) constitute a particularly promising candidate MCM waveform, characterized by its ability to attain maximum spectral efficiency while ensuring very good spectral and temporal confinement [12]. Notably, a guard interval such as a CP is not necessary in a baseline FBMC/OQAM transceiver.

The above advantages of FBMC over OFDM have already been demonstrated and evaluated in terrestrial multiple access scenarios. FBMC-based MA (FBMA) has been shown to be considerably more robust than OFDMA to frequency

V. Dalakas is with the Network Operations Center, Harokopio University of Athens, El. Venizelou 70, 17 671 Athens, Greece (Email: vdalakas@hua.gr).
E. Kofidis is with the Department of Statistics and Insurance Science, University of Piraeus, Piraeus, Greece and the Computer Technology Institute & Press "Diophantus" (CTI), Greece (E-mail: kofidis@unipi.gr).
*Corresponding author: V. Dalakas Tel: +302109549441, Fax: +302109549401, E-mail: vdalakas@hua.gr.

[1]Despite the special nature of the satellite link, there are a number of good reasons for using MCM in satellite transceivers as well [8].

synchronization errors [13], unavoidable in a realistic multi-user environment, especially like the ones envisaged in future mobile networks. Notably, this good behavior is achieved at a much lower cost than in OFDMA [11], both in terms of computation and bandwidth efficiency [14]. In particular, as demonstrated in comparative studies of uplink MA, only a few (theoretically only one) guard (null) subcarriers are needed to ensure minimal inter-user interference in an FBMA system, with OFDMA requiring much wider guard bands to attain a similar performance [15].

Recently, the applicability of FBMC was assessed in a satellite communication context, in the light of the proven effectiveness of FBMC-based MA in 5G scenarios [6], [16]. An important difference with terrestrial systems is the inherently larger difficulty of satellite systems to achieve accurate synchronization among users [2]. In such a setup, and in view of the long and varying signal propagation delays involved, common assumptions made in terrestrial systems are not always easy to be met [17]. Erroneous time synchronization will affect the *orthogonality* of the subcarriers, leading to significant performance degradation due to the presence of inter-block interference (IBI) between successive multicarrier symbols in a multi-user scenario [18]. Moreover, frequency offset errors would require the use of guard bands (GBs) among the subcarriers allocated to each user in a multi-user environment such as the satellite Reverse Link (RL). Another key challenge comes from the use of highly nonlinear power amplifiers (PA) and their effect on the peak-to-average power ratio (PAPR) behavior of MCM schemes.

The authors of [6] have studied the impact of a satellite high-power amplifier (HPA) on OFDM and FBMC in terms of Symbol Error Rate (SER), PAPR and their sensitivity to Carrier Frequency Offset (CFO) in an Additive White Gaussian Noise (AWGN) channel. The two MCM schemes have been found to experience similar spectral regrowth and similar behavior in terms of PAPR. In addition, and as expected, FBMC was demonstrated (through simulations) to be less sensitive to CFO than OFDM [6].[2]

However, the system model considered in [6] does not conform with the DVB-RCS2 family of standards (apart from the employed HPA). Notably, the bit interleaved coding and modulation schemes, e.g., Low-Density Parity-Check (LDPC) and Bose, Chaudhuri, and Hocquenghem (BCH) codes, the transceiver filters and the HPA [2], [20] suggested in DVB-RCS2 differ from the ones commonly adopted so far in related comparative studies [6], [16]. Additionally, on-board HPAs or the ones of the user terminals used in satellite communication systems have highly non-linear transfer functions, including non-linear phase characteristics [21, Chap. 7]. Typically, this is not the case for the PAs employed in their terrestrial counterparts and only the HPAs of the user terminals may share a simplified model, such as the one by Rapp [22]. It must be noted however that even this particular model should be employed in a different manner in the case of a high (> 4) order modulation scheme [23].

[2]A theoretical analysis of the Bit Error Rate (BER) performance of OFDM and FBMC in the presence of an HPA was recently presented in [19].

Motivated by the above, we consider in this paper the application of the aforementioned MA schemes in *state-of-the-art* satellite multi-user systems that are DVB-RCS2-compatible. The two MA MCM schemes are evaluated in an asynchronous multi-user satellite environment considering both potential time- and frequency-domain errors. The figure of merit adopted is the *total degradation (TD)* [8]. It must be emphasized that the aim of this study is to reveal and assess the pros and cons of these transmission technologies in the context of a contemporary satellite standard. Algorithms for compensating related impairments (e.g., [13]) are beyond the scope of this paper.

The rest of the paper is organized as follows. The system model, along with a brief description of OFDM and FBMC/OQAM, is presented in Section II. Performance evaluation results are reported in Section III, where the multi-user performances with and without synchronization errors are evaluated and compared. Conclusions and hints to future related work are given in Section IV.

II. System Model

Fig. 1 depicts the uplink of a typical multi-user satellite communication system. Q users, which may transmit simultaneously, generate independent MA signals, which, after passing through a HPA, are transmitted through the channel. zMA stands for OFDMA or FBMA. In general, the signals arrive at the satellite receiver asynchronously, i.e., with different time or frequency offsets e_q ($1 \leq q \leq Q$). AWGN is assumed to corrupt the received signals. Since both asynchronous, i.e., $e_q \neq 0$, and synchronous, i.e., $e_q = 0, \ \forall\ q$, reception, will be considered, the error blocks shown in Fig. 1 are denoted as optional. As the MA scheme used for downlink might be different from the one employed for the uplink [24], the considered system model assumes that the user signals are demultiplexed and fully recovered at the satellite from the aggregated signal $\mathbf{y}$, observed within a common time interval using Q MA receivers. In the uplink, each User Equipment (UE) multiplexes only its own signal before its HPA (one per user). This procedure is analytically presented in the next section.

A. OFDMA

The OFDMA signal generator consists of a Turbo Encoder (TE), a Modulator (MOD), a Subcarrier Mapping (SM), an M-ary Inverse Discrete Fourier Transform (DFT) (M-IDFT) and a CP adder, with M being the total number of subcarriers forming an OFDM block. The input to the TE consists of random and equally probable bits, a_k, which are encoded by a Turbo code with rate r. The coded bits, b_k, are modulated into the following frequency-domain vector

$$\mathbf{X}_N^q = [X_0, X_1, \ldots, X_n, \ldots, X_{N-1}]^T$$

where $[\cdot]^T$ denotes transposition and the n-th element, X_n, is a complex symbol, which can be selected from a variety of modulation formats. One of the most popular modulation formats, namely 16-QAM, will be considered in our simulations.

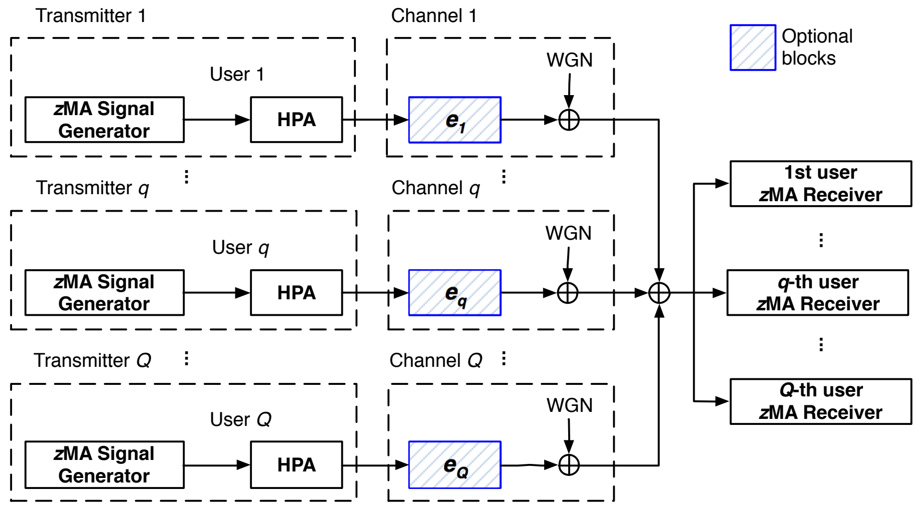

Fig. 1. Model of a satellite uplink.

As each user employs only N out of the M available tones, the remaining $M-N$ tones are set to zero, for example,

$$\mathbf{X}_M^1 = \left[\begin{array}{cc} (\mathbf{X}_N^1)^T & \mathbf{0}_{1\times(M-N)} \end{array} \right]^T \tag{1}$$

for the user $q=1$. In general, the $\mathbf{X}_M^1$ block of symbols is circularly shifted $(q-1)N$ times in order to appropriately position the qth user. In practice, there are virtual (null) subcarriers (VC) located at the edges of the band, say M_{VC} inactive subcarriers. Then $\frac{M_{\text{VC}}}{2}$ zeros are inserted at each of the edges prior to an M-point IDFT that is applied to $\mathbf{X}_M^q$, yielding

$$\mathbf{x}_M^q = \mathbf{F}_M^H \mathbf{X}_M^q \tag{2}$$

where $\mathbf{x}_M^q = [x_0^q, x_1^q, \ldots, x_{M-1}^q]^T$ is the OFDM symbol block of duration T_s, $\mathbf{F}_M$ is the $M \times M$ DFT matrix and $[\cdot]^H$ denotes Hermitian transposition.[3] Denote by $\mathcal{M}^q$ the set of subcarrier indices occupied by user q. Prior to transmission, a CP of length L and duration $T_{\text{CP}} = LT_{\text{s}}/M$, is inserted per OFDM symbol block in order to eliminate the interference between successive MCM symbols. The OFDM symbol after the CP insertion can be conveniently expressed in matrix form as

$$\mathbf{x}_{\text{CP}}^q = \left[\begin{array}{cc} \mathbf{0}_{L\times(M-L)} & \mathbf{I}_L \\ \multicolumn{2}{c}{\cdots\cdots\cdots\cdots\cdots} \\ \multicolumn{2}{c}{\mathbf{I}_M} \end{array} \right] \mathbf{x}_M^q \tag{3}$$

The HPA output signal, $\mathbf{x}_{\text{HPA}}$, can be written as

$$\mathbf{x}_{\text{HPA}}^q = f(\mathbf{x}_{\text{CP}}^q) \tag{4}$$

where $f(\cdot)$ denotes the HPA transfer function. Recall that the signals from each user are corrupted by AWGN and arrive at the satellite with different time or frequency offsets, denoted by e_q $(1 \leq q \leq Q)$.

[3]Of course, the number of available subcarriers is then reduced to $M - M_{\text{VC}}$.

B. FBMA

The FBMC/OQAM-modulated signal of the qth user is given by

$$x^q[l] = \sum_n \sum_{m\in\mathcal{M}^q} d_{m,n}^q p_{m,n}[l], \tag{5}$$

where [25]

$$p_{m,n}[l] = p\left[l - n\frac{M}{2}\right] e^{j\frac{2\pi}{M}m\left(l-\frac{L_p}{2}\right)} e^{j\phi_{m,n}}, \tag{6}$$

with $p[\cdot]$ being the (unit energy and real symmetric) prototype filter impulse response, of length $L_p = KM$, where K is the overlapping factor, and $\phi_{m,n} = (m+n)\frac{\pi}{2} - mn\pi$. The real-valued (pulse amplitude modulated (PAM)) input symbol, $d_{m,n}^q$, resulting from OQAM staggering of the corresponding complex QAM symbol, is transmitted at subcarrier m and at time instant n [25]. The sharing of the frequency spectrum among users is as previously, see (1). Note that no CP is employed in this system. The rest (apart of course from the FBMC/OQAM demodulator) is as in the previous subsection. In our simulations, the prototype filter designed in [26] (and extensively employed in the PHYDYAS project [27]) with $K=3$ was used.

C. Non-linear amplification

According to the DVB-RCS2 implementation guide [23], the non-linear distortion impacting the Return Channel via Satellite Terminal (RCST) transmit Radio Frequencies (RF) signal is mainly caused by the HPA at the UE. It is a common knowledge that the nonlinear characteristics of the HPA depend on several factors, including the technology (i.e., Traveling Wave Tubes Amplifiers (TWTA) vs. Solid State Power Amplifiers (SSPA)), frequency band (e.g., C, Ku or Ka), transmit waveform (modulation scheme and pulse shaping filter), amplifier operating point (input signal level), environment conditions (e.g., temperature) as well as the device aging [23]. The amplitude and phase characteristics of a non-linear device are typically given by the power transfer (AM/AM) and phase transfer (AM/PM) functions that relate the output signal instantaneous power and phase to the input power. Since we consider a multi-user scenario for the RL, the HPA considered here for the UE is an SSPA taken from the standard [23, p. 174]. Its power transfer (AM/AM) characteristic is given by:

$$G(A) = \frac{gA}{\left(1 + (\frac{gA}{A_{\text{sat}}})^{2s}\right)^{\frac{1}{2s}}} \tag{7}$$

where s is the smoothness factor, A_{sat} is the saturation amplitude and g defines the gain of the amplifier in the linear region. This model can be applied to modulated signals as a memoryless function to compute the instantaneous signal amplitude values. Its values have been excerpted from the standard, namely, $s = 6$, $g = 1.122$ and $A_{\text{sat}} = 1.0351$. Asymptotically, the model can present an ideal clipping law (for large values of s).

Please note that, in the open literature, the impact of the phase transfer (AM/PM) characteristic conversion of SSPA on the RF signal is often considered to be negligible. Nevertheless, in the implementation guidelines of the DVB-RCS2, it is recommended for systems that can utilize higher order modulations, particularly 16-QAM, that the phase transfer characteristics of the non-linear device should be examined and considered in system performance evaluation according to phase transfer models provided in [28]. Hence, for a higher accuracy, we have adopted a phase transfer characteristic given by

$$\Phi(A) = \begin{cases} 0, & A < A_{\text{ave}} \\ \alpha\rho(A - A_{\text{ave}}), & A \geq A_{\text{ave}} \end{cases} \tag{8}$$

where ρ is a scaling factor of the slope of AM/PM conversion, A_{ave} is a parameter indicating the point at which the phase rotation starts, and α is a real scalar. The values of these parameters have been excerpted from [28], namely, $\rho = 1$, $\alpha = 0.5259$ and $A_{\text{ave}} = 0.25$.

It should be noted that while there are pre-compensation techniques to be deployed at the transmitter to reduce the impact of such phase (and amplitude) distortions, these are omitted here in order to focus on the clear effect of the impairments on the resulting performance.

D. Classes of users

Fig. 2 illustrates the general case of time asynchronous reception, where the following three distinct classes of users are shown, similarly with [18].

1) Class A: This is the class of *desired* users. It will be henceforth referred to as *Useful Users* (*UU*).
2) Class B: This class includes the asynchronous, with respect to the *UU*, users, which will be referred to as *Other Users* (*OU*).
3) Class C: These are asynchronous with respect to *UU*, which are also contributing IBI. They will be referred to as *IBI Users* (*IBIU*).

In the same figure, the receiver's observation time interval, $T_{\text{R}} = T_{\text{s}} + T_{\text{CP}}$, and its time offsets from the signals of

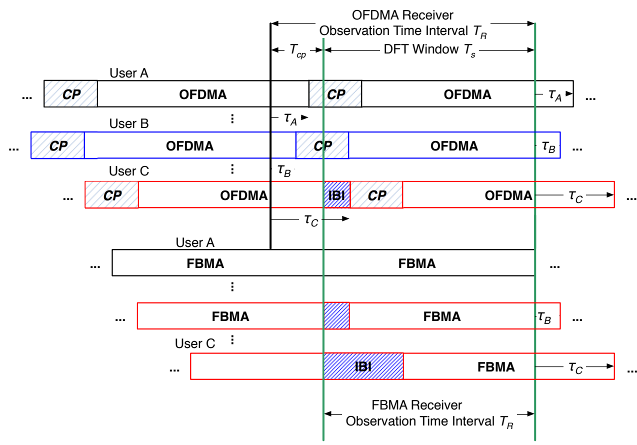

Fig. 2. Schematic of time asynchronous reception. Sequences from OFDMA symbols prefixed with CP are illustrated in relation to the common DFT window of the receiver. Three user classes are illustrated, A, B and C. Note that in FBMA, no CP is used and hence only classes A and C are relevant.

the three classes of users are also indicated. As shown in Fig. 2, since for a C user, the timing offset τ_{C} exceeds the duration of the CP ($T_{\text{CP}} < \tau_{\text{C}}$), IBI will occur. Clearly, as τ_{C} increases, the amount of IBI will also increase. As the other two time offsets (τ_{A} or τ_{B}) do not exceed the duration of the CP, i.e., $0 \leq \tau_{\text{A}}, \tau_{\text{B}} < T_{\text{CP}}$, they do not introduce IBI. Since in our system model the discrete baseband equivalent signal representation is used, these time differences must be represented in discrete form. Hence, the number of samples i, referred to as *IBI factor*, for which the offset exceeds CP, is used to represent the amount of IBI introduced by a C user. Since the duration of a sample is T_{s}/M, the following relation for the delay τ_{C} and the IBI factor i can be written [18]:

$$\begin{aligned} i\frac{T_{\text{s}}}{M} &= \tau_{\text{C}} - T_{\text{CP}} \Rightarrow \\ i &= \left\lceil \frac{M}{T_{\text{s}}}(\tau_{\text{C}} - L\frac{T_{\text{s}}}{M}) \right\rceil \Rightarrow \\ i &= \left\lceil M\frac{\tau_{\text{C}}}{T_{\text{s}}} - L \right\rceil, \end{aligned} \tag{9}$$

where $\lceil a \rceil$ denotes the smallest integer that is not smaller than a. This is not the case for the FBMA transmission, since there is no CP. The receiver's observation time interval is $T_{\text{R}} = T_{\text{s}}$ and, as illustrated in Fig. 2, in the case of asynchronous reception, we always have IBI and Eq. (9) becomes

$$i = \left\lceil M\frac{\tau_{\text{C}}}{T_{\text{s}}} \right\rceil \tag{10}$$

III. Performance Evaluation Results and Discussion

The zMA multi-user communication system under consideration was simulated considering 4 users. The performance evaluation relied on Monte Carlo computer simulations, for three scenarios: ideal reception and erroneous (asynchronous) reception in terms of time offset and frequency offset (CFO). The figure of merit used in the comparison is the Total Degradation (TD) of the two MA schemes. TD is introduced in [29] as a performance criterion indicating how, as compared

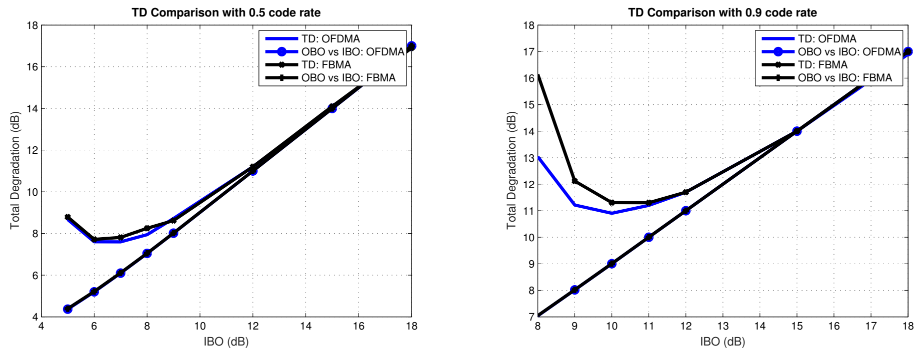

(a) Code rate $r = \frac{1}{2}$

(b) Code rate $r = \frac{9}{10}$

Fig. 3. TD performance of FBMA and OFDMA with perfect reception.

to the linear AWGN channel, the BER performance degrades in the presence of a PA as a function of its operating point (i.e., input back-off (IBO) or output back-off (OBO)). Recall that the OBO is the ratio between the HPA saturation output power point and the operating output power at a given IBO, where IBO is the difference between the operating input power point of the HPA and its saturation point [30]. TD is a generic criterion for evaluating the performance of digital satellite communication systems operating in the presence of an HPA, as it includes the BER performance in its metric [31], [32]. It can be computed as [32]

$$\mathrm{TD} = \frac{E_\mathrm{b}}{N_0}\bigg|^{\mathrm{NL}} - \frac{E_\mathrm{b}}{N_0}\bigg|^{\mathrm{AWGN}} + \mathrm{OBO}. \tag{11}$$

In the above expression, $\frac{E_\mathrm{b}}{N_0}\Big|^{\mathrm{AWGN}}$, where E_b is the energy-per-bit and N_0 the one-sided noise Power Spectral Density (PSD), is the required signal to noise ratio to achieve a target BER in a linear AWGN channel, Similarly, $\frac{E_\mathrm{b}}{N_0}\Big|^{\mathrm{NL}}$ is the required E_b/N_0 for the same target BER taking into account the distortion caused by the HPA operating at a certain OBO. Note that TD, $\frac{E_\mathrm{b}}{N_0}\Big|^{\mathrm{NL}}$, and OBO in (11) are functions of the IBO. Hence, for the sake of clarity, in the following we present TD vs. IBO as well as OBO vs. IBO for each case under consideration.

Considering an AWGN channel, a target BER level must be selected as a point of reference. In our simulations, only the second user belongs to class A (UU) and the remaining 3 users belong to class B (OU). Note that, in FBMA, since no CP is used, the remaining 3 users can only belong to class C (IBIU).

Performance evaluation results have been obtained with an air-interface common in satellite communications. In particular, for the TE, a duo-binary convolutional Turbo code from the DVB-RCS2 standard was selected [33] and the code rate was initially set to $r = \frac{1}{2}$. The modulator formed 16-QAM symbols, while the Max-Log-MAP algorithm [34] with 50 iterations was used to perform hard decoding. Each user block consists of $N = 30$ subcarriers, the length of the IDFT is $M = 128$, with $M_{\mathrm{VC}} = 8$ virtual subcarriers (4 zeros in the beginning and another 4 at the end of the zMA symbol), and the CP length is $L = \frac{M}{8} = 16$. When we have GBs among the users, N is decreased. We have compared FBMA with *no* guard subcarriers against OFDMA with GBs of 0 and 4 subcarriers.

First, it is assumed that each user acquires uplink synchronization at logon. A user terminal acquires frame timing and carrier frequency parameters based on the forward link signal (e.g., 2nd Generation of Digital Video Broadcasting via Satellite (DVB-S2)) at downlink synchronization. It is reasonable to assume that residual frequency errors, with regard to the downlink carrier in the forward link, are smaller than the subcarrier spacing, while residual timing errors with regard to the downlink frame are smaller than the CP duration [18].

To understand the influences of these errors on the two MA schemes, Fig. 3(a) and Fig. 3(b) illustrate their TD performance for two different coding rates, by first considering perfect (i.e., no synchronization errors) on-board reception as a baseline.

Note first that the two MCM schemes have identical OBO vs. IBO performance due to their multi-carrier nature. Moreover, they have almost the same TD minimum when the coding rate equals $r = \frac{1}{2}$, where the TD is around 7.75 dB. With $r = \frac{9}{10}$, OFDMA slightly outperforms FBMA by 0.5 dB.[4]

However, when a time error of 0.1 times the multicarrier symbol duration is considered, FBMA presents a slight improvement of 0.5 dB for low coding rates over its rival (see, e.g., Fig. 4(a)), while it seems that the CP redundancy used in OFDMA renders it more robust than FBMA to time offset errors, as the coding rate increases, but only with a performance gain of 0.25 dB (Fig. 4(b)).

Consider next the case where residual frequency errors are present and assume a CFO equal to half the subcarrier spacing. Fig. 5(a) indicates that FBMA presents a small advantage over its rival, lower than 0.2 dB, when a coding rate of $\frac{1}{2}$ is considered. This performance is reached by OFDMA at the cost of 4 additional guard subcarriers, as illustrated in Fig. 6. This advantage of FBMA is increased as the coding rate is increased, exceeding 0.5 dB as one can observe in Fig. 5(b).

[4]Note that the DVB-RCS2 standard considers a variety of coding rates, ranging from $\frac{1}{2}$ to $\frac{9}{10}$, which justifies our choices.

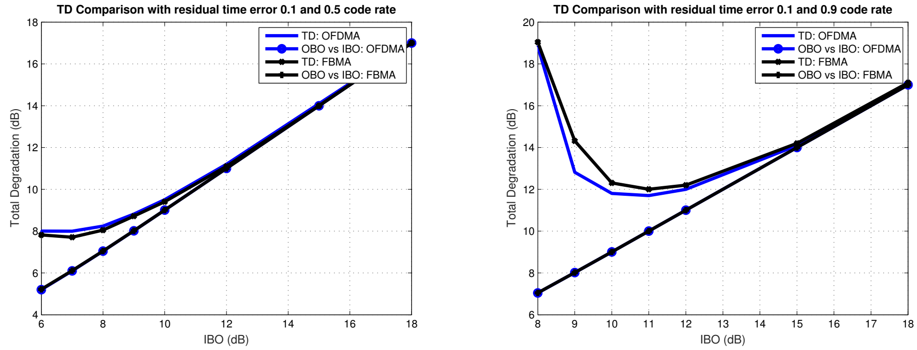

(a) Code rate $r = \frac{1}{2}$ (b) Code rate $r = \frac{9}{10}$

Fig. 4. TD performance of FBMA and OFDMA with a timing error of 0.1 times the multicarrier symbol duration.

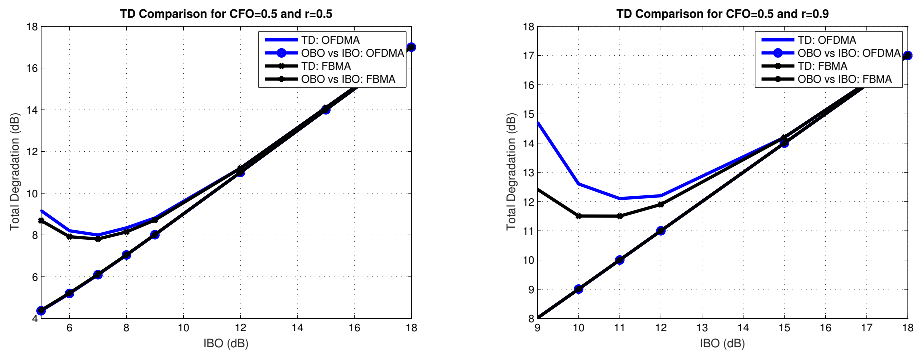

(a) Code rate $r = \frac{1}{2}$ (b) Code rate $r = \frac{9}{10}$

Fig. 5. TD performance of FBMA and OFDMA with a CFO error of half the subcarrier spacing.

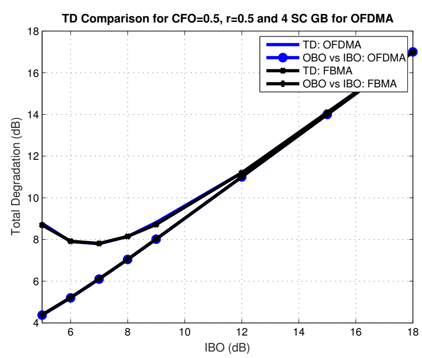

Fig. 6. TD performance of FBMA and OFDMA, with a CFO error of half the subcarrier spacing and 4 guard subcarriers only for OFDMA.

TABLE I
PERFORMANCE RANKING

	Coding Rate r	
	1/2	9/10
Ideal Reception	OFDMA	OFDMA
Time error	FBMA	OFDMA
Frequency error	FBMA	FBMA

Table I presents a summary of the relative ranking of the two MCM MA schemes for the two coding rates considered. FBMA shows advantage in most cases not only in terms of TD but also in terms of spectral efficiency since it does not need any additional guard subcarriers or a CP, while OFDMA seems to prevail only in the presence of time asynchronous reception when a high coding rate is employed.

IV. Conclusions

This paper investigated the applicability of FBMC-based MA in realistic satellite uplink transmission. The OQAM-based FBMC modulation was considered and its performance was compared with that of the classical OFDMA scheme in an air-interface *following the DVB-RCS2 standard*. Both synchronous and asynchronous signal reception were considered. The effect of HPA was taken into account via the employment of an SSPA taken from the DVB-RCS2 standard [23, p. 174], considering also the impact of the phase transfer (AM/PM) characteristic conversion of the SSPA on the RF signal as recommended in the implementation guidelines of DVB-RCS2 and according to the phase transfer models provided in [28]. FBMA was found to be a bit more advantageous in non-ideal reception, particularly at lower coding rates. As expected, in view of the use of a CP, OFDMA showed a higher robustness to time synchronization errors with a high coding rate. However, it was shown to require wider guard bands than FBMA in order to attain a comparable performance in the presence of frequency errors.

Though similar to analogous results presented elsewhere, the results of this study have the additional significance of having being generated for the physical layer of the DVB satellite communications standard, where *coding was also taken into account*. Moreover, the results were expressed here in terms of the TD of the MA schemes under comparison. TD performance curves indicate the optimum (in terms of power efficiency) operating point of the user terminal HPA.

Comparative evaluation results for single-carrier modulation (SCM) OFDM and FBMC MA schemes,[5] will be included in a future version of this work, complementing earlier related studies of MCM vs. SCM OFDMA [17], [18].

References

[1] ETSI, "Digital Video Broadcasting (DVB): Second generation DVB interactive satellite system (DVB-RCS2) Part 2: Lower layers for satellite standard," ETSI, Tech. Rep. EN 101 545-2 v1.1.1, May 2012. [Online]. Available: http://www.etsi.org

[2] P. T. Mathiopoulos, E. A. Candreva, A. B. Awoseyila, V. Dalakas, D. Tarchi, B. G. Evans, A. Vanelli-Coralli, and G. E. Corazza, "Performance improvement techniques for the DVB-RCS2 return link air interface," *International Journal of Satellite Communications and Networking*, vol. 33, no. 5, pp. 371–390, 2015.

[3] T. Guillemin, "Satellites remain key link in evolving hybrid network chain," *Microwave Journal*, pp. 22–30, Aug. 2016.

[4] A. Kyrgiazos, B. Evans, P. Thompson, P. T. Mathiopoulos, and S. Papaharalabos, "A Terabit/second satellite system for European broadband access: a feasibility study," *International Journal of Satellite Communications and Networking*, vol. 32, no. 2, pp. 63–92, 2014. [Online]. Available: http://dx.doi.org/10.1002/sat.1067

[5] "TERASAT - Approaching the Terabit/s satellite: a system study." [Online]. Available: http://telecom.esa.int/telecom/www/object/index.cfm?fobjectid=31254

[6] J. Dommel, G. Boccolini, L. Raschkowski, S. Jaeckel, L. Thiele, T. Haustein, and N. G. Prelcic, "5G in space: PHY-layer design for satellite communications using non-orthogonal multi-carrier transmission," in *7th Advanced Satellite Multimedia Systems Conference and the 13th Signal Processing for Space Communications Workshop (ASMS/SPSC)*, Sept. 2014, pp. 190–196.

[7] P. Banelli *et al.*, "Modulation formats and waveforms for 5G networks: Who will be the heir of OFDM?" *IEEE Signal Process. Mag.*, vol. 31, no. 6, pp. 80–93, Nov. 2014.

[8] A. Ginesi and F. Potevin, "OFDM digital transmission techniques for broadband satellites," in *24th AIAA International Communications Satellite Systems Conference*, San Diego, CA, June 2006.

[9] ETSI, "Digital Video Broadcasting (DVB): Framing Structure, channel coding and modulation for Satellite Services to Handheld devices (SH) below 3 GHz," Tech. Rep. EN 302 583 v1.0.0, December 2007. [Online]. Available: http://www.etsi.org

[10] 3GPP, 3rd Generation Partnership Project, "Technical Specification Group Radio Access Network; Evolved Universal Terrestrial Radio Access (E-UTRA); Physical Layer Procedures (Release 11)," Tech. Rep. TS 36.213, 2013. [Online]. Available: http://www.etsi.org

[11] M. Morelli, C.-C. Kuo, and M.-O. Pun, "Synchronization techniques for orthogonal frequency division multiple access (OFDMA): A tutorial review," *Proc. IEEE*, vol. 95, no. 7, pp. 1394–1427, July 2007.

[12] B. Farhang-Boroujeny, "OFDM vs. filter bank multicarrier," *IEEE Signal Process. Mag.*, vol. 28, no. 3, pp. 92–112, May 2011.

[13] G. J. González, F. H. Gregorio, J. Cousseau, R. Wichman, and S. Werner, "Uplink CFO compensation for FBMC multiple access and OFDMA in a high mobility scenario," *Physical Communication*, vol. 11, pp. 56–66, 2014. [Online]. Available: http://dx.doi.org/10.1016/j.phycom.2013.10.002

[14] H. Saeedi-Sourck, Y. Wu, J. W. M. Bergmans, S. Sadri, and B. Farhang-Boroujeny, "Complexity and performance comparison of filter bank multicarrier and OFDM in uplink of multicarrier multiple access networks," *IEEE Trans. Signal Process.*, vol. 59, no. 4, pp. 1907–1912, April 2011.

[15] B. Doré, V. Berg, N. Cassiau, and D. Kténas, "FBMC receiver for multi-user synchronous transmission on fragmented spectrum," *EURASIP Journal on Advances in Signal Processing*, 2014. [Online]. Available: http://asp.eurasipjournals.com/content/2014/1/41

[16] S. Dimitrov *et al.*, "Disruptive satellite broadband radio interface design," Broadband Access via integrated Terrestrial and Satellite systems (BATS project), Deliverable D4.4.2, 2015. [Online]. Available: http://www.batsproject.eu/images/PublicDeliverables/BATS_D4.4.2_DLR_v1_F.pdf

[17] S. Rosati, G. Corazza, and A. Vanelli-Coralli, "Orthogonal multicarrier modulations in satellite uplinks," *International Journal of Satellite Communications and Networking*, vol. 32, pp. 213–224, 2014.

[18] V. Dalakas, P. T. Mathiopoulos, F. Di Cecca, and G. Gallinaro, "A comparative study between SC-FDMA and OFDMA schemes for satellite uplinks," *IEEE Trans. Broadcast.*, vol. 58, no. 3, pp. 370–378, Sept. 2012.

[19] H. Bouhadda, H. Shaiek, D. Roviras, R. Zayani, Y. Medjahdi, and R. Bouallegue, "Theoretical analysis of BER performance of nonlinearly amplified FBMC/OQAM and OFDM signals," *EURASIP Journal on Advances in Signal Processing*, vol. 2014, no. 1, pp. 1–16, 2014.

[20] V. Dalakas, S. Papaharalabos, P. Mathiopoulos, E. Candreva, G. Corazza, and A. Vanelli-Coralli, "BICMC and TD comparative performance study of 16-APSK signal variants for DVB-S2 systems," *IEEE Commun. Lett.*, vol. 19, no. 5, pp. 723–726, May 2015.

[21] G. E. Corazza, Ed., *Digital Satellite Communications*. New York, NY: Springer, 2007.

[22] C. Rapp, "Effects of HPA-nonlinearity on a 4-DPSK/OFDM-signal for a digital sound broadcasting system," in *2nd European Conference on Satellite Communications (ECSC-1991)*, Liege, Belgium, October 1991, pp. 179–184.

[23] DVB, "DVB-RCS2 lower layer satellite implementation guidelines," ETSI, Tech. Rep. Blue Book A162, Feb 2013. [Online]. Available: http://www.dvb.org

[24] ETSI, "Digital Video Broadcasting (DVB): Second generation framing structure, channel coding and modulation system for broadcasting, interactive services, news gathering and other broadband satellite applications," Tech. Rep. EN 302 307 v1.1.2, June 2006. [Online]. Available: http://www.etsi.org

[25] P. Siohan, C. Siclet, and N. Lacaille, "Analysis and design of OFDM/OQAM systems based on filterbank theory," *IEEE Trans. Signal Process.*, vol. 50, no. 5, pp. 1170–1183, May 2002.

[26] M. G. Bellanger, "Specification and design of a prototype filter for filter bank based multicarrier transmission," in *Proc. ICASSP-2001*, Salt Lake City, UT.

[27] ——, "FBMC physical layer: A primer," Tech. Rep., 2010, PHYDYAS project report. [Online]. Available: http://www.ict-phydyas.org/teamspace/internal-folder/FBMC-Primer_06-2010.pdf

[28] M. Ichikawa, T. Hara, M. Saito, M. Okada, and H. Yamamoto, "Evaluation of BER degradation due to phase nonlinearity of SSPA on MC-CDMA signals," in *2005 IEEE International Conference on Personal Wireless Communications (ICPWC-2005)*, Jan. 2005, pp. 533–536.

[29] A. D'Andrea, V. Lottici, and R. Reggiannini, "RF power amplifier linearization through amplitude and phase predistortion," *IEEE Trans. Commun.*, vol. 44, no. 11, pp. 1477–1484, Nov. 1996.

[30] M. Aloisio, E. Casini, and A. Ginesi, "Evolution of space traveling-wave tube amplifier requirements and specifications for modern communication satellites," *IEEE Trans. Electron Devices*, vol. 54, no. 7, pp. 1587 –1596, July 2007.

[31] ETSI, "Guidelines for the implementation and use of EN 301 545-2 (DVB-RCS2 Lower Layer)," Tech. Rep. 101 545-4 V1.1.1, April 2014.

[32] R. De Gaudenzi, A. Guillen, and A. Martinez, "Performance analysis of turbo-coded APSK modulations over nonlinear satellite channels," *IEEE Trans. Wireless Commun.*, vol. 5, no. 9, pp. 2396–2407, Sep. 2006.

[33] ETSI, "Digital Video Broadcasting (DVB); Interaction channel for satellite distribution systems," ETSI, Tech. Rep. EN 301 790 v1.3.1, Mar 2003. [Online]. Available: http://www.etsi.org

[34] S. Papaharalabos, P. T. Mathiopoulos, G. Masera, and M. Martina, "On optimal and near-optimal turbo decoding using generalized $\max^*$ operator," *IEEE Commun. Lett.*, vol. 13, no. 7, pp. 522–524, 2009.

[5] more suitable for uplink transmission